Cyclic Fasting–Mimicking Diet Plus Bortezomib and Rituximab Is an Effective Treatment for Chronic Lymphocytic Leukemia

Franca Raucci[1], Claudio Vernieri[1,2], Maira Di Tano[1,3], Francesca Ligorio[1,2], Olga Blaževitš[1], Samuel Lazzeri[1], Anastasiya Shmahala[1], Giuseppe Fragale[1], Giulia Salvadori[1], Gabriele Varano[1], Stefano Casola[1], Roberta Buono[4,5], Euplio Visco[1], Filippo de Braud[2,6], and Valter D. Longo[1,5]

ABSTRACT

Cyclic fasting–mimicking diet (FMD) is an experimental nutritional intervention with potent antitumor activity in preclinical models of solid malignancies. FMD cycles are also safe and active metabolically and immunologically in cancer patients. Here, we reported on the outcome of FMD cycles in two patients with chronic lymphocytic leukemia (CLL) and investigated the effects of fasting and FMD cycles in preclinical CLL models. Fasting-mimicking conditions in murine CLL models had mild cytotoxic effects, which resulted in apoptosis activation mediated in part by lowered insulin and IGF1 concentrations. In CLL cells, fasting conditions promoted an increase in proteasome activity that served as a starvation escape pathway. Pharmacologic inhibition of this escape mechanism with the proteasome inhibitor bortezomib resulted in a strong enhancement of the proapoptotic effects of starvation conditions *in vitro*. In mouse CLL models, combining cyclic fasting/FMD with bortezomib and rituximab, an anti-CD20 antibody, delayed CLL progression and resulted in significant prolongation of mouse survival. Overall, the effect of proteasome inhibition in combination with FMD cycles in promoting CLL death supports the targeting of starvation escape pathways as an effective treatment strategy that should be tested in clinical trials.

Significance: Chronic lymphocytic leukemia cells resist fasting-mimicking diet by inducing proteasome activation to escape starvation, which can be targeted using proteasome inhibition by bortezomib treatment to impede leukemia progression and prolong survival.

Introduction

Cyclic fasting and fasting-mimicking diets (FMD) have been consistently found to promote additive or synergistic antitumor effects when combined with standard anticancer treatments in murine models of human malignancies, including melanoma, breast, colorectal, and lung cancer (1–6). In patients with cancer, cyclic FMD is safe and well tolerated when combined with standard antineoplastic therapies, and it also results in metabolic modifications, such as a reduction of blood glucose, insulin, and insulin-like growth factor 1 (IGF1) concentration, which recapitulate metabolic changes responsible for the antitumor effects of nutrient starvation in preclinical experiments (3, 4, 7–9). In addition, recent clinical reports have shown that combining cyclic FMD with chemotherapy, endocrine therapies, or immunotherapy improves tumor responses in patients with early-stage neoplasms, and it induced complete and long-lasting tumor remissions in some patients with highly aggressive advanced malignancies (3, 9–11).

While solid preclinical and preliminary clinical evidence supports the anticancer effects of cyclic calorie restriction in different models of solid neoplasms, the anticancer activity of cyclic fasting/FMD in chronic leukemias has been poorly investigated.

Chronic lymphocytic leukemia (CLL) is the most common type of leukemia in Western countries (12–14). CLL is highly heterogeneous from a biological and clinical point of view, with some patients presenting with an indolent disease that progresses slowly, while patients with aggressive CLL undergo fast accumulation of leukemic lymphocytes in the bone marrow and in lymphoid tissues, where they replace normal hematopoietic cells, finally resulting in blood cytopenia. Indolent CLL is usually addressed with a "watch and wait" strategy, whereas pharmacologic treatments are initiated in case of clinical evolution, including the onset of thrombocytopenia, anemia, a rapid increase of lymphocyte counts, or lymph node/organ involvement.

The clinical armamentarium against CLL has dramatically expanded in the last decade, and it includes cytotoxic compounds, such as nucleoside analogues (fludarabine) or alkylating agents (cyclophosphamide, chlorambucile, bendamustine; refs. 15–17), and targeted therapies, such as the anti-CD20 mAbs rituximab, ofatumumab and obinituzumab (18–20), the Bruton tyrosine kinase (BTK) inhibitors ibrutinib, zanubrutinib, and acalabrutinib (21–24) and the BCL2 inhibitor venetoclax (25, 26). Despite this remarkable therapeutic progress, new safe and effective CLL treatments are needed in both first-line treatment setting and in subsequent lines of therapy, especially for patients with more aggressive disease course, such as patients with CLL bearing 17p deletion/*TP53* mutations. Among experimental drugs, the proteasome inhibitors bortezomib and carfilzomib have recently shown promising anti-CLL activity (27–29).

[1]IFOM ETS, the AIRC Institute of Molecular Oncology, Milan, Italy. [2]Medical Oncology Department, Fondazione IRCCS Istituto Nazionale dei Tumori, Milan, Italy. [3]Weill Cornell Medical College, Department of Medicine, Cornell University, New York, New York. [4]Department of Molecular Biology and Biochemistry, University of California, Irvine, Irvine, California. [5]Longevity Institute, Davis School of Gerontology and Department of Biological Sciences, University of Southern California, Los Angeles, California. [6]Department of Oncology and Hemato-Oncology, University of Milan, Milan, Italy.

F. Raucci and Claudio Vernieri contributed equally to this article.

Corresponding Author: Valter D. Longo, Longevity Institute, Davis School of Gerontology and Department of Biological Sciences, University of Southern California, Los Angeles, CA 90089. E-mail: vlongo@usc.edu

Cancer Res 2024;84:1133–48

doi: 10.1158/0008-5472.CAN-23-0295

Because dysregulated systemic glucose and lipid metabolism is a risk factor for CLL development (30, 31), and because cyclic FMD is emerging as a safe and effective anticancer strategy in several human malignancies (3, 7–10), we investigated whether cyclic calorie restriction has therapeutic potential against CLL. We show that cyclic fasting or FMD has mild anti-CLL effects when used alone in CLL mouse models and in patients with cancer, while cyclic FMD in combination with bortezomib and rituximab delays CLL progression through apoptosis activation, resulting in meaningful survival prolongation of CLL-bearing mice.

Materials and Methods

FMD in patients

In this study, we reported on two patients with CLL enrolled in the NCT03340935 trial, which investigated the safety, feasibility, metabolic, and immunologic effects of cyclic FMD in a heterogeneous population of patients with cancer treated with concomitant antitumor therapies. Results of the NCT03340935 trial have been recently published (7). In brief, the FMD regimen used in the NCT03340935 trial consisted in 5-day, plant-based, low-calorie (a maximum of 600 Kcal on day 1, and a maximum of 300 Kcal on days 2–5), low-carbohydrate, low-protein diet that was repeated every 21–28 days, up to a maximum of 8 consecutive cycles. Patient compliance to the FMD was assessed through daily food diaries that were filled by patients and analyzed by the investigators at the end of each FMD cycle. Patients enrolled in the trial underwent blood and urine collection and analysis at the initiation and at the end of each FMD cycle to count peripheral blood cells and to measure metabolic parameters. The studies were conducted in accordance with one of the following ethical guidelines: Declaration of Helsinki, International Ethical Guidelines for Biomedical Research Involving Human Subjects (CIOMS), Belmont Report. The study protocol was approved by the Institutional Review Board and by the Ethics Committee of Fondazione IRCCS Istituto Nazionale dei Tumori. Enrolled patients provided a written informed consent to take part in the trial, and for the use of clinical and biological data for research purposes. In the interval between consecutive FMD cycles, patients were recommended to adhere to International guidelines for cancer prevention and for cancer survivors (American Cancer Society 2012).

Cell lines and culture conditions

MEC1, MEC2 human chronic B cell leukemia cell lines, and L-1210 murine chronic lymphocytic leukemia cell line were purchased from Deutsche Sammlung von Mikroorganismen und Zellkul- turen (DMSZ). BJ normal fibroblast cell line derived from human foreskin and 3T3-NIH normal fibroblast cell line derived from murine embryo were purchased from ATCC. All cell lines were maintained in DMEM (Life Technologies, catalog no. 10566) supplemented with 10% FBS (Biowest, catalog no. S1810), 1% nonessential amino acids (Biowest, catalog no. X-0557), and 1% penicillin/streptomycin (Biowest, catalog no. L0022). All cells were tested for *Mycoplasma* contamination routinely. Cells were maintained in a humidified, 5% CO_2 atmosphere at 37°C.

In *in vitro* experiments, the control medium (CTRL) consisted of a glucose-free DMEM, which was supplemented with 1 g/L of glucose and 10% FBS. Short-term starvation (STS) consisted of DMEM without glucose (DMEM no glucose, Life Technologies, catalog no. 11966025), which was then supplemented with 0.25 g/L glucose (Sigma-Aldrich, catalog no. G8769) and 1% FBS, thus resulting in 75% and 90% reduction of glucose and FBS concentration, respectively, when compared with the CTRL medium.

For rescue experiments, cells were cultured under CTRL, STS, STS + 1 g/L glucose + 1% FBS (to specifically evaluate the effect of FBS restriction), STS + 0.25 g/L glucose + 10% FBS (to specifically evaluate the effect of glucose restriction), or STS + 0.25 g/L glucose + 1% FBS + individual FBS growth factors at physiologic concentrations [IGF1: 250 ng/mL (PeproTech, catalog no. 100–11), insulin: 200 ng/mL (Sigma-Aldrich, catalog no. 11376497001), and IGF1 inhibitor: 100 nmol/L (BMS-754807, catalog no. S1124] for a total of 48 hours.

In vitro cell viability assays

CLL (MEC1, MEC2 and L1210) and normal (BJ and 3T3NIH) cell lines were seeded in 12-well plates in control (10% FBS, 2 g/L glucose for human cell lines) or starvation medium (0.5 g/L glucose, 1% FBS); 24 hours after plating, cells were treated with different chemical compounds for 24 hours. At the end of the experiment (48 hours after plating), cell viability and cell death were assessed by erythrosine B exclusion assay. Briefly, cells were seeded in 12-well plates (250,000 cells per well); 24 hours after seeding, cells were rinsed twice in PBS, and then grown in CTRL or STS medium. After 24 hours, growth media were refreshed to ensure that glucose and serum levels were not completely exhausted and, after pH stabilization at 37°C and 5% CO_2 atmosphere, cells were treated with different chemical compounds, including bortezomib (10 nmol/L), rituximab (1μg/mL) or vehicle, for 24 hours. Then, cells were harvested, centrifuged, and resuspended, for a final concentration of 1×10^6 cells per mL. Details regarding "Reagent preparation," "Cell viability assays," "Apoptosis evaluation through Annexin V and propidium iodide (PI) staining by FACS analysis," "Cell cycle study by PI staining and FACS analysis," "Cell viability upon bortezomib treatment in medium supplemented human serum," and "Proteasome activity assay" are detailed in Supplementary Methods.

Mouse experiments and diet

Mouse experiments were performed in accordance with guidelines established in the Principles of Laboratory Animal Care (directive 86/609/EEC), and they were approved by the Italian Ministry of Health. NOD SCID gamma (NSG) mice were acquired from Charles Rivers Laboratories. Mice were maintained in a pathogen-free environment and housed in air-filtered laminar flow cabinets with a 12-hour light cycle and food and water *ad libitum*. Mice were acclimatized for 2 weeks. A total of 1×10^{11} MEC1 cells were injected intravenously or subcutaneously (in left flank) in 8- to 12-week-old female NOD SCID gamma (NSG) mice. Dietary regimens used in mouse experiment are described in Supplementary Methods.

Fasting/FMD cycles and pharmacologic treatments were initiated 6 days and 10 days after intravenous or subcutaneous tumor cell injection, respectively. In each experiment, mice were randomly assigned to one of six arms (with $n = 8$–10 mice per treatment arm): (i) control: *ad libitum* standard diet; (ii) fasting (48 hours); (iii) bortezomib (0.35 mg/kg) + rituximab (10 mg/kg) and standard diet; (iv) bortezomib (0.35 mg/kg) + rituximab (10 mg/kg) and fasting; (v) FMD; (vi) bortezomib (0.35 mg/kg) + rituximab (10 mg/kg) and FMD regimen. Bortezomib and rituximab were administered intraperitoneally, once per week for 3 weeks. In fasting cohorts, pharmacologic treatments were performed 24 hours after fasting initiation, while in FMD groups treatments were administered after 48 hours of diet regimen.

Subcutaneous tumor volume estimation

The volume of subcutaneous tumor masses was calculated using the formula: $(w^2 \times W) \times \pi/6$, where "$w$" and "$W$" are tumor minor and major diameters (in mm), respectively. The maximal tumour volume

that was permitted by our Institutional Animal Care and Use Committee was 1,500 mm^3, and this limit was never exceeded in our experiments. Mice were sacrificed by CO_2 inhalation after three weeks of treatment immediately after the end of the third fasting cycle. Organs were isolated and were formalin-fixed for histologic analyses. Cells from peritoneal exudates, blood, bone morrow, and spleen were isolated for subsequent flow cytometry analyses. For survival experiments, only intravenous model was applied and mice treated weekly FMD, for a total of 5 cycles.

Details regarding "Histological and immunofluorescence," as well as "Flow cytometry," are described in Supplementary Methods.

Statistical analysis

GraphPad Prism v8.0.2 (159) and R Studio (v2022.02.3) were used for the analysis of the data and graphic representations. Comparisons between groups were performed with two-sided unpaired Student *t* test, with the exception of clinical data analysis, in which paired Wilcoxon test was used to compare lymphocyte counts before and after subsequent FMD cycles in patients with cancer. One-way ANOVA analysis was used for comparison among multiple groups for mouse experiments. One-way ANOVA analysis was followed by Tukey posttest analysis. *P* values ≤ 0.05 were considered as statistically significant. For the design of *in vivo* experiments, we calculated the sample size by G.Power software according to multifactorial variance analysis. We obtained that $n = 10$ mice per group could reach a power of 0.9 (subject to alpha = 0.05). We checked the presence of outliers, which were removed according to ROUT method (ROUT = 1%). A confidence interval of 95%, corresponding to *P* value ≤ 0.05 for two-tailed statistical comparisons, was considered significant. For survival analysis, the log-rank (Mantel–Cox) test was performed. All data were represented as mean ± SEM of at least three independent experiments.

Data availability statement

All raw data generated in the study are available upon request from the corresponding authors.

Results

Five-day FMD reduces lymphocyte counts in patients with CLL

Among 101 patients enrolled in the NCT03340935 phase Ib trial (7), two patients had CLL.

Patient 1 is a 62-year-old male, who was diagnosed B-type, Rai stage II CLL bearing 13q deletion (FISH analysis) in 2011. Baseline CT and ^{18}FDG Positron Emission Tomography (^{18}FDG-PET) showed multiple pathologic supradiaphragmatic and subdiaphragmatic lymph nodes (including retro-pancreatic, paraaortic, neck lymph nodes up to a maximum diameter of 3.5 cm). The patient was approached through a "watch and wait" strategy, with a progressive increase of peripheral blood lymphocytes until January 2017 (28,800/μL), when he was deemed eligible to receive first-line bio-chemotherapy (**Fig. 1A**). In February 2017, the patient decided to postpone the initiation of systemic treatments, and since November 2016 he reduced daily calorie intake, which led to a meaningful reduction of blood lymphocytes (**Fig. 1A**). In March 2017, the patient was enrolled in the NCT0334093 trial, and he started 5-day FMD cycles every-28-days without concomitant antineoplastic therapies. The patient tolerated well eight consecutive FMD cycles, that is, the maximum number of FMD cycles allowed as per NCT03340935 trial protocol. Blood glucose and insulin concentration was reduced after the FMD, while urinary ketone bodies were increased (**Fig. 1A**), thus reproducing metabolic changes recently reported in the whole NCT03340935 trial cohort (7). The patient underwent consistent, yet reversible reduction of peripheral blood lymphocyte counts during most FMD cycles, with overall reduced lymphocyte counts at the end of eight FMD cycles as compared with the pre-FMD period (**Fig. 1B**). Moreover, the patient experienced progressive reduction in the volume of palpable lymph nodes (i.e., supraclavicular and lateral cervical lymph nodes). In December 2022, that is, 70 months after FMD initiation, the patient remains under clinical observation, with slow but progressive increase of peripheral blood lymphocyte counts that has not required the initiation of systemic treatments yet.

Patient 2 is a 57-year-old male with Rai stage 0 CLL diagnosed in January 2018 after the occasional finding of peripheral blood absolute (10,400 cells/μL) and relative (70%) lymphocytosis (**Fig. 1C**). B lymphocytes ($CD19^+$) accounted for 78% of all lymphocytes and had a $CD5^+/CD19^+/CD23^+/CD20^+$(dim)/$CD38^-$ phenotype. The monoclonal immunoglobulin heavy chain (*IGHV*) gene was found to be rearranged, while cytogenetic analysis of CLL cells revealed chromosome 12 trisomy. No enlargement of superficial or profound lymph nodes and spleen was detected by physical or ultrasound examination of the abdomen. The patient was a candidate to a "watch and wait" strategy. In February 2018, he was enrolled in the NCT03340935 trial and started every-21-days FMD cycles without concomitant medical treatments. The patient tolerated well eight consecutive FMD cycles, with a reduction of blood glucose, insulin, and IGF1 concentration after most FMD cycles (**Fig. 1C**). Peripheral blood lymphocyte counts underwent a reduction during most FMD cycles (**Fig. 1D**). Despite a trend toward a progressive increase in lymphocyte counts over the time (**Fig. 1D**), no pharmacologic treatments have been initiated so far (i.e., 58 months after FMD initiation).

To understand whether the observed reduction of peripheral blood lymphocytes after 5-day FMD also occurs in patients with other malignancies, we studied the kinetics of blood lymphocytes in 26 patients who underwent cyclic FMD, alone ($n = 6$) or in combination with radiotherapy ($n = 1$) or systemic treatments other than chemotherapy, namely endocrine therapy ($n = 13$), immunotherapy ($n = 3$), nuclear therapy ($n = 1$), or targeted therapies ($n = 2$), in the context of the NCT03340935 trial. In this analysis, we excluded patients treated with concomitant chemotherapy, which could *per se* reduce blood lymphocyte counts, thus resulting in confounding results. As shown in Supplementary Fig. S1, in these 26 patients, we did not observe a reduction of peripheral blood lymphocytes after each of several consecutive FMD cycles, thus suggesting that FMD may cause a long-lasting reduction of leukemic lymphocytes, but not normal lymphocytes. This result is consistent with a large body of preclinical evidence showing that nutrient starvation can selectively reduce the proliferation or survival of tumor cells while activating protective responses in normal cells (1, 32, 33).

Together, data from patients enrolled in the NCT03340935 trial indicate that cyclic FMD, as used without concomitant antitumor therapies, can reversibly reduce the number of peripheral blood lymphocytes. Although these patients experienced a progressive increase of blood lymphocyte counts over the years, none of them necessitated the initiation of pharmacologic treatments so far.

Starvation has mild *in vitro* anti-CLL effects

To assess which FMD-induced metabolic changes are responsible for the reduction of peripheral blood lymphocyte counts, in *in vitro* experiments we assessed the impact of starvation conditions (STS) on the *in vitro* mortality of two human CLL cell lines, namely MEC1 and MEC2 cells. These two cell lines have been derived from the same patient with CLL, but they were collected during different phases of the

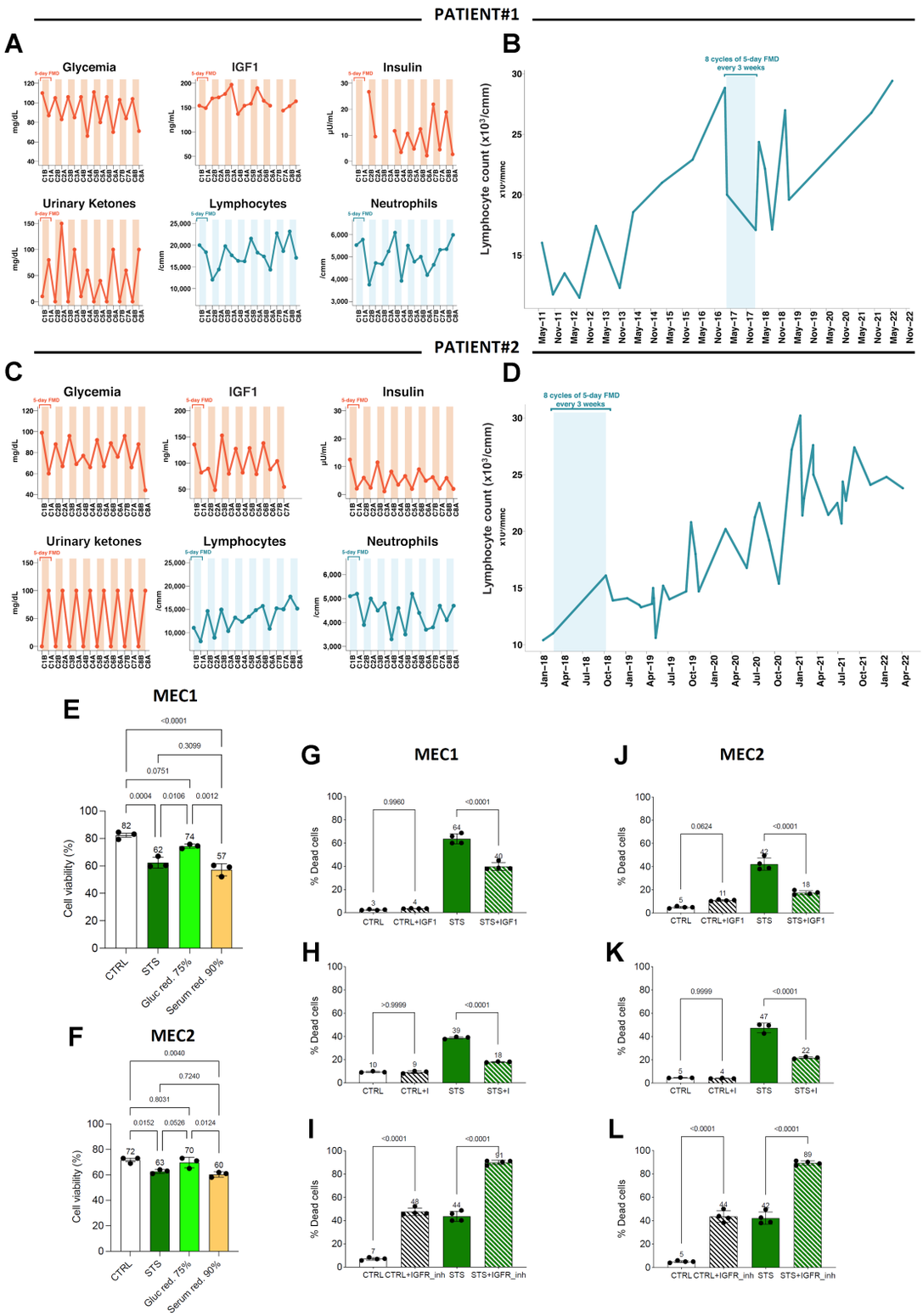
PATIENT#1
A
Glycemia
IGF1
Insulin
Urinary Ketones
Lymphocytes
Neutrophils
B
8 cycles of 5-day FMD every 3 weeks
Lymphocyte count (x10³/cmm)
PATIENT#2
C
Glycemia
IGF1
Insulin
Urinary ketones
Lymphocytes
Neutrophils
D
8 cycles of 5-day FMD every 3 weeks
Lymphocyte count (x10³/cmm)
E
MEC1
Cell viability (%)
CTRL
STS
Gluc red. 75%
Serum red. 90%
F
MEC2
Cell viability (%)
G
MEC1
% Dead cells
CTRL
CTRL+IGF1
STS
STS+IGF1
H
% Dead cells
CTRL
CTRL+I
STS
STS+I
I
% Dead cells
CTRL
CTRL+IGFR_inh
STS
STS+IGFR_inh
J
MEC2
% Dead cells
K
% Dead cells
L
% Dead cells

course of the disease (34, 35). Consistent with previously published data, we confirmed by Sanger sequencing that both MEC1 and MEC2 cells harbor the homozygous insertion c.949_950insC in *TP53* (36). Then, we asked whether glucose or serum restriction mostly contributes to STS-induced anti-CLL effects. As shown in **Fig. 1E** and **F**, serum restriction, but not glucose restriction, was responsible for STS-induced increase of cell mortality in both MEC1 and MEC2 cells. On the basis of this result, we hypothesized that the restriction of specific growth factors that are contained in the serum, such as insulin or IGF1, may be responsible for STS cytotoxic effects. In line with this hypothesis, the supplementation of IGF1 or insulin reduced or reversed STS-induced anti-CLL effects (**Fig. 1G**, **H**, **J**, and **K**), while pharmacologic inhibition of IGF1 receptor (IGFR1) significantly increased STS-induced CLL cell mortality (**Fig. 1I**, and **L**). Together, these data suggest that FMD-induced reduction of IGF1 and insulin contributes to its anti-CLL effects, likely by inhibiting insulin receptor (IR) and IGF1R signaling in CLL cells.

CLL cells activate the proteasome as an adaptive mechanism to STS

To identify new starvation-based anti-CLL treatment combinations to be tested *in vivo*, we screened 15 chemical compounds, including some cytotoxic and molecularly targeted agents that are active against CLL (Supplementary Table S1), for their ability to enhance STS-induced cell mortality in MEC1 and MEC2 cells, as well as in the murine L1210 CLL line (p53-defective; ref. 37). Among these compounds, the proteasome inhibitor bortezomib increased the mortality of MEC1, MEC2, and L1210 cells when used alone and, more importantly, it resulted in the strongest synergistic antileukemic effects when combined with STS (**Fig. 2A**–**C**). These results were replicated in MEC1 and MEC2 cells previously adapted to grow in a medium containing human serum, which has different composition, in terms of concentration of growth factors and other metabolites, when compared with the FBS (Supplementary Fig. S2A and S2B). While STS and bortezomib cooperated to increase CLL cell mortality, STS rescued the proapoptotic effect of bortezomib in two nontransformed cell lines, namely human BJ and murine 3T3-NIH fibroblasts (Supplementary Fig. S2C–S2F, respectively), thus expanding previous data on the protective effects of starvation conditions against the effects of toxic chemicals in normal cells (1, 3, 38).

To explain the cooperative anti-CLL effects of STS and bortezomib, we hypothesized that CLL cells exposed to STS boost proteasomal activity as a prosurvival mechanism. To test this hypothesis, we measured proteasomal activity in MEC1 and MEC2 cells exposed to STS. In line with our hypothesis, STS caused a major increase in proteasome activity after 24 hours in MEC1 cells, while in MEC2 cells STS-induced proteasome activation was even more precocious (3 hours), and it was maintained after 6 and 24 hours (**Fig. 2D** and **E**). As expected, bortezomib alone strongly inhibited proteasome activity. Of note, bortezomib completely reversed STS-induced increase of proteasome activity (**Fig. 2D** and **E**). STS-induced increase in proteasome activity is unlikely to be mediated by changes in the expression of proteasome subunits; indeed, Western blot analysis showed that the proteasome subunits USP-14, PSMD4, PSMD7, and PSMD14 are not significantly modulated by STS, bortezomib, or STS + bortezomib when compared with CTRL conditions (Supplementary Fig. S3A and S3B).

Because STS consists of a combination of serum restriction and glucose restriction, we investigated which of these two starvation components is mostly responsible for the observed boost in proteasomal activity. Consistent with the preminent role of serum restriction in mediating STS-induced an increase of CLL cell mortality (**Fig. 1E** and **F**), serum restriction, but not glucose restriction, contributed to increase proteasomal activity in MEC1 and MEC2 cells (**Fig. 2F** and **G**).

To understand whether an enhanced proteasome activation is a general response of neoplastic cells to nutrient starvation or, alternatively, if it specifically occurs in CLL cells, we exposed two human breast cancer models, namely MCF7 (hormone receptor-positive breast cancer cells that are sensitive to growth factor restriction (3) and SUM159PT (human triple-negative breast cancer cells that are sensitive to glucose deprivation (4) cells, to STS conditions. As shown in Supplementary Fig. S3C and S3D nutrient starvation did not result in an increase in proteasome activity in these cells, and in SUM159PT cells it even induced a decrease in proteasome activity. Therefore, the effects of STS on enhanced proteasome activation do not apply to all cancer types, and they seem to be specific for CLL cells.

Impact of STS and bortezomib on cell-cycle progression and apoptosis

To investigate the mechanisms through which STS and bortezomib, alone or in combination with rituximab, cooperate to reduce CLL cell viability, we studied the impact of these treatments on cell-cycle progression through FACS-mediated evaluation of PI incorporation in fixed MEC1 cells previously exposed to CTRL, STS, bortezomib, rituximab, STS + rituximab, STS + bortezomib, bortezomib + rituximab, or STS + bortezomib + rituximab conditions for 36, 42, or 48 hours. As shown in **Fig. 3A**–**C** (see in Supplementary Fig. S4A–S4C exemplifying distributions for these treatment conditions at each timepoint), STS or rituximab did not significantly affect cell-cycle progression, whereas bortezomib resulted in cell accumulation in the G_2–M phase, likely by preventing the degradation of cyclin B1 and

Figure 1.

FMD reduces lymphocyte counts in CLL patients and it has mild anti-CLL effects in *in vitro* models by acting through the IGF axis. **A–D,** Kinetics of peripheral blood lymphocytes, neutrophils, and metabolic parameters (blood IGF1, glucose, and insulin, and urinary ketone bodies) in two patients with CLL undergoing 8 FMD cycles in the NCT03340935 trial. **A** and **C** illustrate long-term lymphocyte kinetics to include the timeframes before and after the dietary intervention. During FMD, blood and urine samples were collected at the initiation and at the end of each FMD cycle to measure the concentration of plasma glucose, serum insulin/IGF1, urinary ketone bodies, as well as total neutrophil and lymphocyte counts (**B** and **D**). C1B, cycle 1, before FMD; C1A, cycle 1, after FMD; C2B, cycle 2, before FMD; C2A, cycle 2, after FMD; C3B, cycle 2, before FMD; C3A, cycle 3, after FMD; C4B, cycle 4, before FMD; C4A, cycle 4, after FMD; C5B, cycle 5, before FMD; C5A, cycle 5, after FMD; C6B, cycle 6, before FMD; C6A, cycle 6, after FMD; C7B, cycle 7, before FMD; C7A, cycle 7, after FMD; C8B, cycle 8, before FMD; C8A, cycle 8, after FMD. **E** and **F,** Effects of glucose (Gluc red., 75%) or serum (Serum red., 90%) restriction on the viability of MEC1 (**E**) and MEC2 (**F**) cells cultured in control (CTRL), STS medium, glucose-restricted medium (75% of glucose reduction as compared with CTRL medium), or serum restricted medium (90% of serum reduction as compared with CTRL medium). Data are presented as the mean ± SD of three independent experiments ($n = 3$). Statistical significance was determined using a one-way ANOVA test with Tukey post hoc analysis. *, $P < 0.05$; **, $P < 0.01$; ***, $P < 0.001$; ns, not significant. **G–L,** Effects of IGF1/insulin supplementation and IGFR1 inhibition on the viability of MEC1 (**G–I**) and MEC2 (**J–L**) cells cultured in CTRL and STS medium, alone or in combination with IGF, the IGFR1 inhibitor BMS-754807, or insulin. Bar plots indicate the percentage of dead cells at the end of the experiments, and the percentage of dead cells in each replicate is indicated by a single point. The test of proportions was used to compare the ratio of dead cells with or without the IGFR1 inhibitors in each treatment condition.

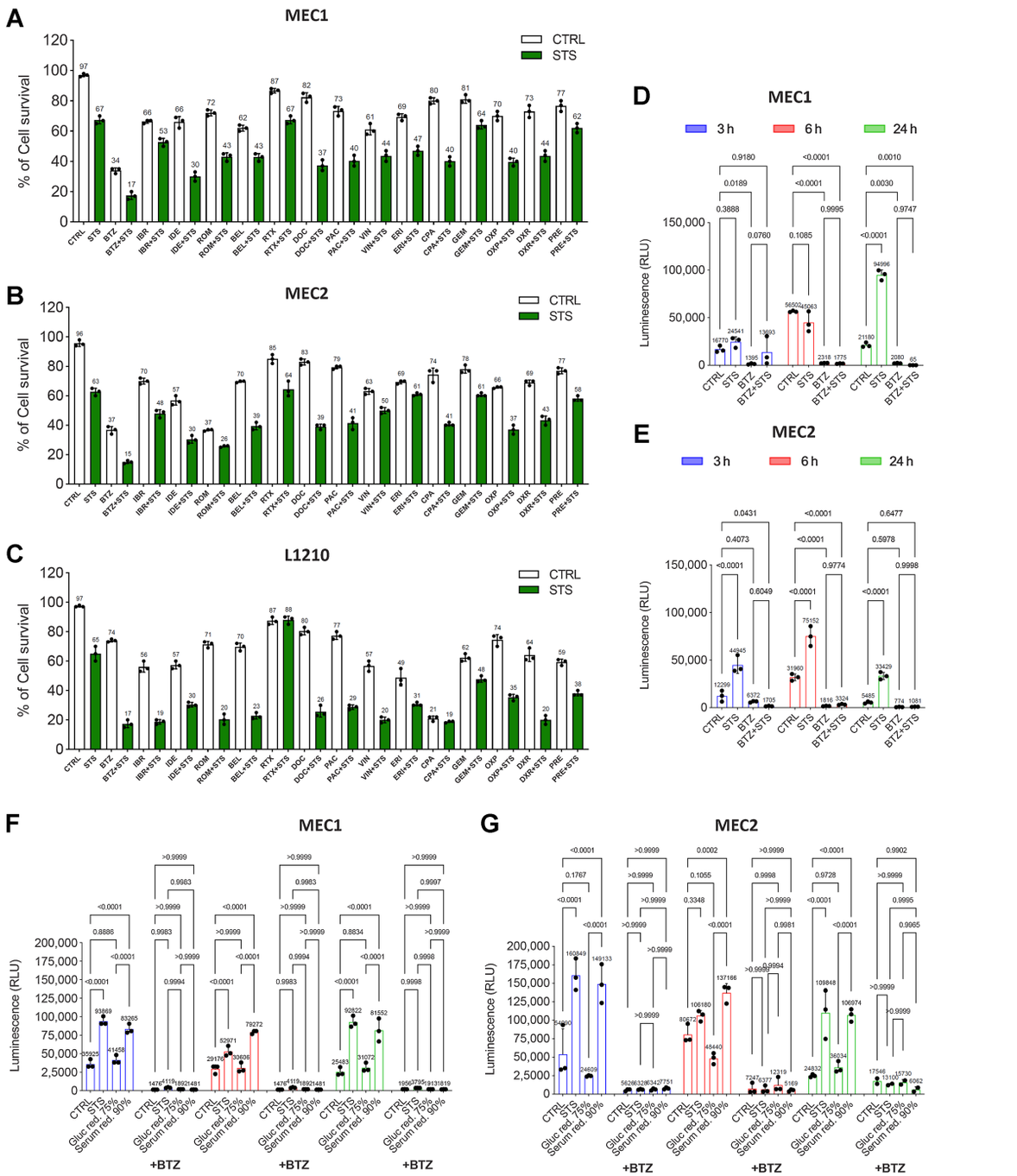

Figure 2.

STS activates the proteasome as an adaptive resistance mechanism. **A–C,** Survival rates of MEC1 (**A**), MEC2 (**B**), and L1210 (**C**) cells cultured in CTRL and STS medium, alone or in the presence of the indicated drugs. Cell survival was measured by erythrosine B exclusion assay. CTRL, physiological condition; BTZ, bortezomib (10 nmol/L); IBR, ibrutinib (5 μmol/L); IDE, idelalisib (50 μmol/L); ROM, romodepsin (10 ng/mL); BEL, belinostat (50 μmol/L); RTX, rituximab (1 μg/mL); DOC, docetaxel (10 μmol/L); PAC, paclitaxel (10 μmol/L); VIN, vincristine (250 nmol/L); doxorubicin (1 μmol/L); ERI, eribulin (10 μmol/L); CPA, cyclophosphamide (100 μmol/L); GEM, gemcitabine, (5 μmol/L); OXP, oxaliplatin (2 μmol/L); DXR, dexamethasone, (100 μmol/L); PRE, prednisone (10 μg/mL). Results from three independent experiments. Data are expressed as mean ± SD. **D** and **E,** Proteasome activity in MEC1 (**D**) and MEC2 (**E**) cells cultured in CTRL and STS medium, alone or in the presence of bortezomib. Bortezomib, 10 nmol/L. Results from three independent experiments are shown. Data are expressed as mean ± SD. **F** and **G,** Impact of glucose restriction (75% of glucose compared with CTRL medium) or serum restriction (90% of serum compared to control medium) on the proteasome activity in MEC1 (**F**) and MEC2 (**G**) cells cultured in four different conditions, with or without bortezomib. Gluc red., glucose restricted; Serum red., serum restricted. Data are presented as the mean ± (SD) of three independent experiments ($n = 3$). Statistical significance was determined using a two-way ANOVA test with Tukey post hoc analysis. *, $P < 0.05$; **, $P < 0.01$; ***, $P < 0.001$; ns, not significant.

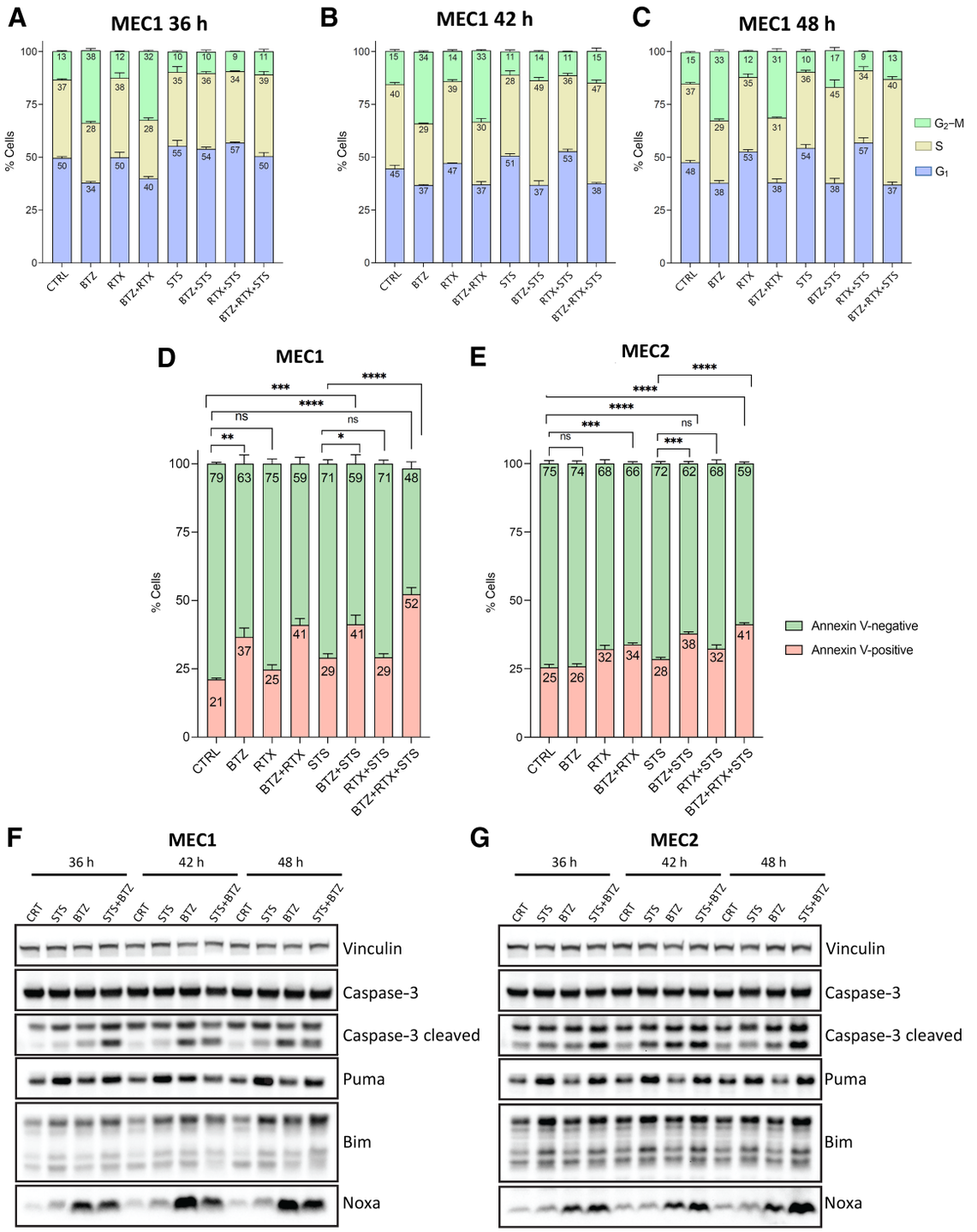

Figure 3.

Impact of STS and bortezomib on cell-cycle progression and apoptosis. **A–C,** Cell-cycle analysis using PI staining and flow cytometry. **A,** Cell-cycle distribution of MEC1 cells treated with CTRL, STS, bortezomib (BTZ), rituximab (RTX), STS + rituximab, STS + bortezomib, bortezomib + rituximab, or STS + bortezomib + rituximab for 36 hours, as assessed by FACS analysis of PI incorporation. **B,** Cell-cycle distribution analysis after 42 hours of treatment. **C,** Cell-cycle distribution analysis after 48 hours of treatment. Data are presented as mean ± SD of three independent experiments. **D** and **E,** Proapoptotic effects of STS, bortezomib, or STS + bortezomib, alone or in combination with rituximab, in MEC1 and MEC2 cells. The percentage of Annexin V–positive (apoptotic) cells among total cancer cells was quantified by FACS analysis at 36 hours in MEC1 cells (**D**) and MEC2 cells (**E**) after exposure to the indicated treatments. Data are presented as mean ± SEM of three independent experiments. **F** and **G,** Western blot analysis of the expression of caspase-3, cleaved caspase-3, Noxa, PUMA, and BIM protein levels in MEC1 (**F**) and MEC2 (**G**) cells exposed to STS, bortezomib, or their combination, compared to with untreated control cells. Western blot data were replicated in tso independent experiments. Vinculin was used as a protein loading control.

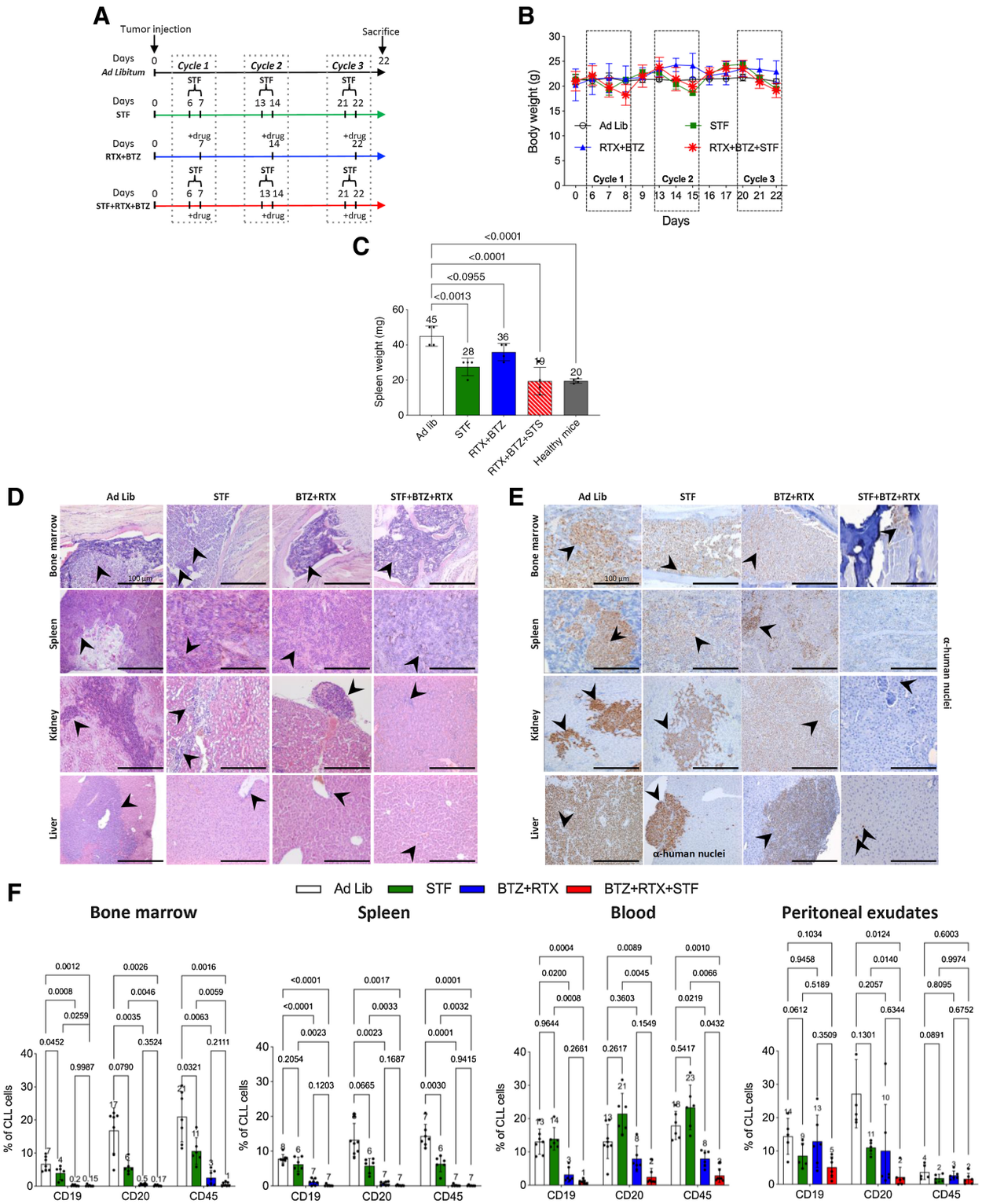

Figure 4.

Cyclic fasting synergizes with bortezomib (BTZ)-rituximab (RTX) to retard CLL progression. **A,** Experimental scheme of fasting and BTX in an intravenous mouse CLL model (MEC1 cells). Three cycles of each of the indicated treatments were administered. **B,** Body weight (g) modifications over the time and under the indicated treatment conditions are represented. (*Continued on the following page.*)

retarding exit from mitosis (39). Interestingly, STS reversed bortezomib-induced G_2–M arrest (**Fig. 3A–C**), thus suggesting that bortezomib-induced mitotic arrest is not crucial for the cooperative anti-CLL effect of STS and bortezomib. On the other hand, rituximab, either alone or in combination with STS, bortezomib, or STS + bortezomib, did not significantly affect cell-cycle progression (**Fig. 3A–C**).

Then, we asked whether starvation conditions result in apoptosis activation in CLL cells. In *in vitro* experiments, we assessed apoptosis by FACS analysis through the quantification of the percentage of Annexin V–positive cells at 36 hours after treatment initiation (Supplementary Fig. S5A and S5B). As shown in **Fig. 3D** and **E**, STS caused a mild increase in the percentage of Annexin V–positive (apoptotic) cells in both cell lines, which became more pronounced when bortezomib was combined with STS. In line with these data, Western blot analysis revealed an increase in the expression of several apoptotic markers, such as cleaved caspase-3, Puma, Bim, Noxa in MEC1 and MEC2 cells exposed to STS (as compared with cells treated with CTRL conditions; **Fig. 3F** and **G**). Of note, combining bortezomib and STS resulted in a stronger increase in the expression of cleaved caspase-3 and Bim (**Fig. 3F** and **G**). Interestingly, when compared with the STS + bortezomib doublet, the STS + bortezomib + rituximab triple treatment caused a larger increase in the percentage of Annexin V–positive cells (**Fig. 3D** and **E**), thus suggesting that rituximab boosts the proapoptotic *in vitro* effects of the STS + bortezomib combination through tumor cell–autonomous mechanisms. These effects could in part be mediated by bortezomib-induced increase in CD20 expression, while combining rituximab with bortezomib fully reverses this effect (Supplementary Fig. S5C).

Together, these data indicate that STS activates apoptosis in CLL cells, whereas bortezomib, either alone or in combination with rituximab, enhances these proapoptotic effects.

Cyclic fasting synergizes with bortezomib–rituximab to retard CLL progression

On the basis of *in vitro* data showing synergistic cytotoxic effects of STS and bortezomib in CLL models, we investigated the antitumor activity of combining cyclic fasting with BTZ in an *in vivo*, intravenous mouse model of CLL, which recapitulates the systemic nature of CLL in humans (32, 40).

Because anti-CD20 mAbs are commonly used as part of polypharmacologic combinations for CLL treatment, and based on *in vitro* experiments showing an increase in the proportion of apoptotic cells when rituximab is combined with STS + bortezomib (**Fig. 3D** and **E**), in *in vivo* experiements we used the bortezomib–rituximab combination as a pharmacologic backbone to be tested either alone or in combination with nutrient starvation. Eight-week-old NODSCID ilrg$^{-/-}$ female mice were injected 1×10^7 MEC1 cells via lateral tail veins. Six days after injection, mice were randomly allocated to one of four experimental groups (9 mice per group): *ad libitum* diet without pharmacologic treatments (control group), cyclic fasting, here indicated as short-term fasting or STF (48 hours of water-only fasting followed by 5-day refeeding, up to a maximum of three fasting cycles), bortezomib + rituximab, or STF + bortezomib + rituximab (**Fig. 4A**). At the end of the experiment, peripheral blood, peritoneal exudates, and organs (bone marrow, spleen, kidneys, and liver) were collected. Animals treated with STF or STF + bortezomib + rituximab underwent reversible reduction of body weight, but complete weight recovery occurred after 24–48 hours of refeeding (**Fig. 4B**). Mice in the control group underwent progressive enlargement of the spleen, which indicates CLL progression as a result of spleen colonization by leukemic lymphocytes. Notably, STF significantly reduced spleen weight, while STF plus bortezomib–rituximab led to complete reversion of splenomegaly, that is, reaching a size similarly to that in control healthy mice of the same age (**Fig. 4C**).

To assess the infiltration of peripheral organs by CLL cells, we evaluated the presence of leukemic lymphocytes in hematoxylin/eosin (H&E)-stained tumor sections from these organs. In mice fed with *ad libitum* diet, we observed either a diffuse lymphocyte infiltration pattern, or focal discrete aggregates of medium-to-large leukemic lymphocytes with clumped chromatin and round nucleoli in bone marrow, spleen, liver, and kidney (**Fig. 4D**). Both STF and bortezomib + rituximab, when used alone, resulted in a reduction of organ-infiltrating lymphocytes. The STF + bortezomib+ rituximab combination caused a more evident decrease of lymphocyte infiltration in bone marrow and spleen, with no residual infiltrating lymphocytes observed in the liver and in the kidney (**Fig. 4D**; Supplementary Fig. S6A shows H&E sections of the same organs in healthy mice). IHC analysis using a human anti-nuclei antibody recognizing human cells (Supplementary Fig. S6B) confirmed a significant reduction of leukemic lymphocytes in the bone marrow, spleen, kidney, and liver of mice treated with STF + bortezomib + rituximab as compared with mice receiving STF or bortezomib + rituximab alone (**Fig. 4E**). To confirm these data, we quantified by FACS analysis the proportion of cells expressing human CLL markers, that is, human CD19, CD20, and CD45, in cell suspensions of bone marrow, spleen, peripheral blood, and peritoneal exudates collected from animals (40). Antibody specificity and cross-reactivity was evaluated in MEC1 cells (positive control; Supplementary Fig. S6C) and in tissues from mice not injected with MEC1 cells (negative control; Supplementary Fig. S6D). In line with previous data, cyclic STF significantly reduced CD19$^+$, CD20$^+$, and CD45$^+$ leukemic cells in all these organs (**Fig. 4F**). Bortezomib + bortezomib had potent antileukemic effects, leading to a significant reduction of CD19$^+$, CD20$^+$, and CD45$^+$ cells in peripheral blood and peritoneal exudates, and to an almost complete clearance of leukemic cells in the bone marrow and in the spleen (**Fig. 4F**). However, the STF + bortezomib + rituximab combination resulted in an almost complete clearance of leukemic cells in all

(*Continued.*) **C,** Spleen weight (mg) modifications over the time, and under the indicated treatment conditions, are represented. **D,** H&E staining of bone marrow, spleen, kidney, and liver. Ad lib + Vehicle, $N = 8$; STF + vehicle, $N = 6$; BTZ+RTX: Ad lib + bortezomib (0.35 mg/kg) + rituximab (10 mg/kg) once a week for 3 weeks (days 7, 14, 21), $N = 7$; STF + bortezomib +rituximab: Fasting + bortezomib (0.35 mg/kg once a week) + rituximab (10 mg/kg) once a week for 3 weeks (days 7, 14, 21), $N = 7$. Each treatment was administered for three cycles. Black arrows, lymphocytes. Scale bar, 100 μm **E**, Immune staining of several mouse tissues through anti-human nuclei antibody: eight-week-old NODSCID ilrg$^{-/-}$ female mice were injected intravenously with MEC1 cells, and the indicated tissues were collected and stained to identify the presence of human cells (leukemic lymphocytes; black arrows). Scale bar, 100 μm. Ad lib + vehicle, $N = 8$; STF = fasting + vehicle, $N = 6$; bortezomib + rituximab = Ad lib + bortezomib (0.35 mg/kg) + rituximab (10 mg/kg) once a week for 3 weeks (days 7, 14, 21), $N = 7$; STS + bortezomib + rituximab = fasting + bortezomib (0.35 mg/kg once a week) + rituximab (10 mg/kg) once a week for 3 weeks (days 7, 14, 21), $N = 7$. **F,** Effect of STF, bortezomib–rituximab, or their combination on CLL cell infiltration of the bone marrow, spleen, blood, and peritoneal exudates, as evaluated by FACS analysis. At the end of experimental procedures, cells collected from different organs or tissues were analyzed by flow cytometry after staining with mAb directed against human CD19, CD20, and CD45, respectively, to identify leukemic B-cell population. Ad lib + Vehicle, $N = 7$; STF = fasting + vehicle, $N = 6$; bortezomib + rituximab = Ad lib + bortezomib (0.35 mg/kg) + rituximab (10 mg/kg) once a week for 3 weeks (days 7, 14, 21), $N = 7$; STF + BTZ + RTX = fasting + bortezomib (0.35 mg/kg once a week) + rituximab (10 mg/kg) once a week for 3 weeks (days 7, 14, 21), $N = 7$.

organs and tissues evaluated, including the blood and peritoneal exudates (**Fig. 4F**).

Together, these data indicate that cyclic STF retards the progression of an *in vivo* model of murine CLL, and that it cooperates with bortezomib + rituximab to reduce leukemia cell number in many organs.

Cyclic fasting and bortezomib–rituximab cooperate in retarding the growth subcutaneous CLL masses

While the intravenous CLL model more reliably recapitulates the systemic nature of human CLL, subcutaneous CLL models allow timely measurement of tumor mass volumes and an assessment of the antitumor activity of experimental therapies. To establish a subcutaneous xenograft mouse model of CLL, we injected 1×10^7 of MEC1 cells into the left flank of eight-week-old NODSCID ilrg$^{-/-}$ female mice (40). Approximately 10 days after tumor cell injection (i.e., when tumor volume was 135 ± 49.5 mm^3), mice ($n = 9$) were randomly assigned to one of the following treatment groups: *ad libitum* diet, STF, bortezomib + rituximab or STF + bortezomib + rituximab (Supplementary Fig. S6E). Fasted animals reversibly lost 10%–15% of their weight, which fully recovered upon refeeding (Supplementary Fig. S6F). When used alone, STF or rituximab–bortezomib similarly reduced tumor volume when compared with tumors from mice in the *ad libitum* group. Of note, combining cyclic STF and rituximab–bortezomib caused additive antitumor effects, with an average, 2-fold reduction of tumor volume at the end of the experiment (**Fig. 5A–C**). In mice fed *ad libitum*, tumor masses showed some central necrosis embedded in larger areas of viable tumor cells. STF and, more evidently, the STF + bortezomib + rituximab combination, resulted in major modifications of tumor tissue architecture and integrity, with large and disseminated necrotic and apoptotic areas (**Fig. 5D**). IHC analysis performed in formalin-fixed, paraffin-embedded tumor specimens collected at the end of the experiment revealed an increase in the expression of cleaved caspase-3 in tumor masses from animals treated with STF or bortezomib + rituximab when compared with the control group; notably, the STF + bortezomib + rituximab triplet resulted in a more significant increase in cleaved caspase-3 levels when compared with single treatments (**Fig. 5E**), which is consistent with the results of *in vitro* experiments (**Fig. 3F** and **G**). Together, these data indicate cooperative effects of STF and bortezomib + rituximab in activating apoptosis and in retarding the progression of subcutaneous CLL models, with a reduction of CLL masses and a retardation of CLL metastatic spread to distant organs.

Cyclic FMD in combination with bortezomib–rituximab prolongs animal survival in systemic CLL mouse model

While water-only fasting is poorly applicable in the clinic, cyclic FMDs are emerging as a safe, well-tolerated, and potentially active nutritional intervention when used in combination with standard therapies in patients with cancer (7, 8, 41). To increase the translatability of our previous findings, we investigated whether fasting-induced enhancement of bortezomib + rituximab antitumor activity can be reproduced by a more clinically feasible cyclic FMD. To this aim, in the intravenous CLL model (MEC1 cells), animals were randomly allocated to *ad libitum* diet without pharmacologic treatments (control group), cyclic FMD, bortezomib + rituximab, or FMD + bortezomib + rituximab (Supplementary Fig. S7A). FMD-induced reduction of animal body weight (∼16%) was recovered after 24 hours of refeeding (Supplementary Fig. S7B). When used alone, FMD or bortezomib + rituximab reduced spleen weight, while the FMD + bortezomib + rituximab combination showed a trend toward an additional reduction in splenomegaly (**Fig. 6A**). Three cycles of 72-hour FMD, or the bortezomib + rituximab combination, significantly reduced the number of leukemic lymphocytes in bone marrow, spleen, peripheral blood, and peritoneal exudates (**Fig. 6B**). Notably, the FMD + bortezomib + rituximab combination almost completely cleared malignant lymphocytes in all organs and tissues analyzed (**Fig. 6B**). The cooperative antileukemic effects of FMD and bortezomib + rituximab were especially evident in peripheral blood and peritoneal exudates (**Fig. 6B**). H&E analyses confirmed that FMD + bortezomib + rituximab reduces organ-infiltrating lymphocytes when compared with CTRL, FMD alone, or bortezomib + rituximab (**Fig. 6C**).

To investigate the effect of cyclic FMD plus bortezomib + rituximab on animal survival, we performed a similar experiment, but with longer treatment duration. In particular, bortezomib was administered up to a maximum of 5 cycles, while rituximab and FMD were continued until excessive toxicity or animal death/sacrifice. Despite a reduction of organ-infiltrating lymphocytes, cyclic FMD was not potent enough to prolong animal survival when used alone (**Fig. 6D**), thus suggesting that the anti-CLL activity of cyclic FMD is not long-lasting, in line with what was observed in patients with CLL (**Fig. 1A–D**). On the other hand, bortezomib + rituximab prolonged animal survival when compared with CTRL and cyclic FMD alone (**Fig. 6D**). Of note, combining cyclic FMD and bortezomib + rituximab resulted in statistically significant increase of animal survival when compared with cyclic FMD or bortezomib–rituximab (**Fig. 6D**). Together, these data indicate that cyclic FMD and bortezomib + rituximab not only cooperate in reducing organ infiltration by leukemic lymphocytes and in retarding CLL progression, but they also result in meaningful prolongation of animal survival.

Discussion

Periods of fasting/FMDs slow down tumor growth and synergize with standard antineoplastic treatments, including endocrine therapies, targeted therapies or immunotherapy, in both tumor-bearing mice and in patients with cancer (1–6, 9). In a recent work, cyclic fasting without concomitant pharmacologic treatments inhibited the development and progression of acute lymphoblastic leukemia (ALL), but not of acute myeloid leukemia (AML), through the modulation of the Leptin Receptor (LEPER) pathway (42).

Here, based on anecdotal evidence that cyclic FMD in the absence of concomitant pharmacologic treatments reversibly reduced peripheral blood lymphocyte counts in two patients with CLL, we studied the effect of cyclic fasting/FMD in mouse CLL models. We provide strong evidence that fasting and FMD cycles slow down the progression of both intravenous and subcutaneous CLL mouse models by activating apoptosis in CLL cells as a result of reduced concentrations of blood growth factors, such as insulin and IGF1. However, the anti-CLL effects of cyclic fasting/FMD are transient, and cyclic FMD does not impact on the long-term disease course. This could be in part due to the ability of CLL cells to activate proteasome activity as an adaptive resistance mechanism to starvation, in agreement with our recent results in triple-negative breast cancer models in which cancer cells activated various starvation escape pathways that could be pharmacologically targeted toinduce durable tumor regression (4). Indeed, combining cyclic fasting/FMD with the proteasome inhibitor bortezomib and anti-CD20 mAbs cooperatively slowed down the progression of both

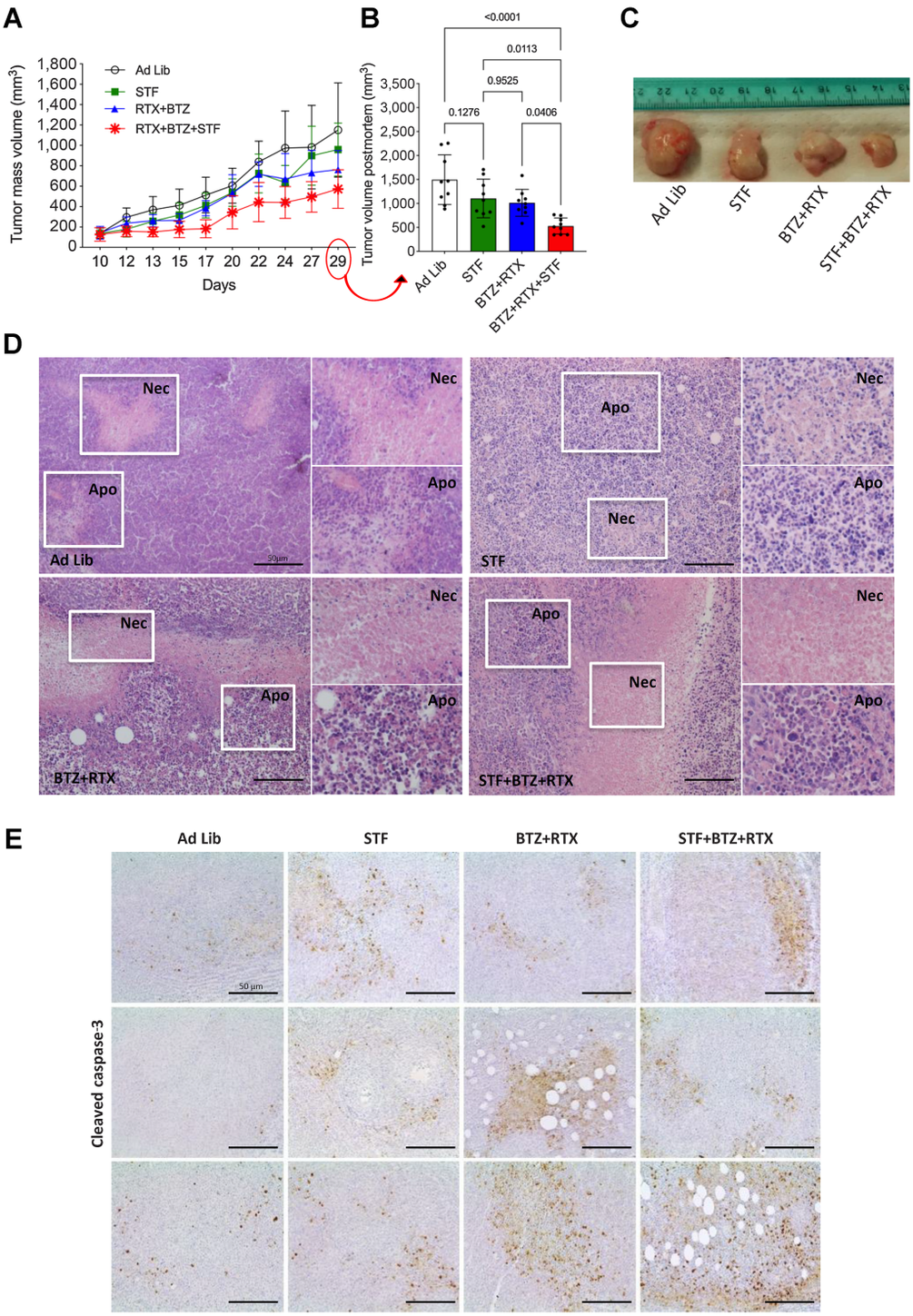

Figure 5.

Cyclic fasting and bortezomib + rituximab cooperate in retarding the growth of subcutaneous CLL masses. **A,** Experimental scheme of cyclic fasting and bortezomib (BTZ) + rituximab (RTX) in subcutaneous mouse CLL model (MEC1 cells). Each of the indicated treatments was administered for three cycles. **B,** Bar plots representing the volume of subcutaneous tumor masses collected at the end of the experiment and estimated through the formula indicated in Materials and Methods. **C,** Picture of some tumor masses after dissection. **D,** H&E-stained tumor sections from subcutaneous tumor masses explanted at the end of the experiment. Necrotic (Nec) and/or apoptotic areas (Apo) are visible in all experimental group (white boxes and higher magnifications). Scale bar, 50 µm. **E,** IHC analysis of cleaved caspase-3 expression in tumor masses collected at the indicated time points from animals exposed to the indicated treatment conditions. Three pictures are shown for each treatment condition.

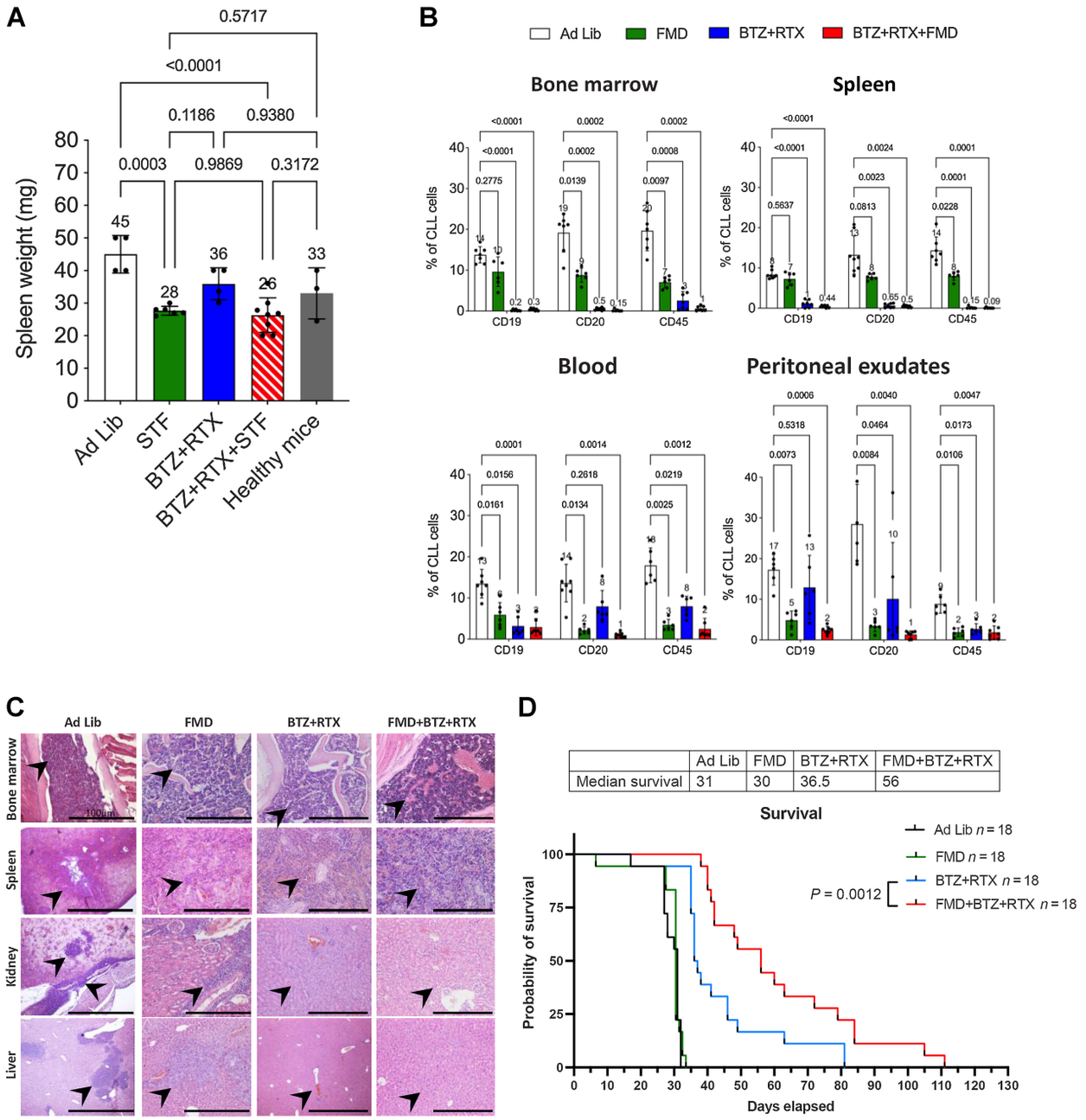

	Ad Lib	FMD	BTZ+RTX	FMD+BTZ+RTX
Median survival	31	30	36.5	56

Figure 6.

Cyclic FMD plus bortezomib + rituximab retards CLL progression in an intravenous CLL model. **A,** Spleen weight (mg) modifications over the time and under the indicated treatment conditions are represented. **B,** Effect of FMD, bortezomib + rituximab, or their combination, on the percentage of CLL cells in the bone marrow, spleen, blood and peritoneal exudates, as evaluated by FACS analysis. At the end of experimental procedures, cells collected from the indicated organs or tissues were analyzed by flow cytometry after staining with mAb against human CD19, CD20, and CD45 to identify leukemic B cell populations. Ad lib + Vehicle, $N = 8$; FMD: Fasting-mimicking diet + vehicle, $N = 6$; bortezomib + rituximab: Ad lib + bortezomib (0.35 mg/kg) + rituximab (10 mg/kg) once a week for 3 weeks (days 7, 14, 21), $N = 7$; FMD + bortezomib + rituximab: FMD + bortezomib (0.35 mg/kg once a week) + rituximab (10 mg/kg) once a week for 3 weeks (days 7, 14, 21), $N = 7$. **C,** H&E staining of bone marrow, spleen, kidney, and liver. Ad lib + Vehicle, $N = 8$; FMD: + vehicle, $N = 6$; bortezomib + rituximab: Ad lib + bortezomib (0.35 mg/kg) + rituximab (10 mg/kg) once a week for 3 weeks (days 7, 14, 21), $N = 7$; FMD + bortezomib + rituximab: fasting + bortezomib (0.35 mg/kg once a week) + rituximab (10 mg/kg) once a week for 3 weeks (days 7, 14, 21), $N = 7$. Each treatment was administered for three cycles. Black arrows and higer magnifications indicate hematoxylin-positive lymphocytes. Scale bar, 100 µm. **D,** Kaplan–Meier survival curves of mice randomly allocated to *ad libitum* diet (CTRL, $N = 18$), cyclic FMD ($N = 18$), bortezomib + rituximab ($N = 18$), or cyclic FMD+ bortezomib + rituximab ($N = 18$) in an intravenous CLL murine model. Bortezomib was administered up to a maximum of 5 cycles. FMD and rituximab were administered until unacceptable toxicities or animal death/sacrifice.

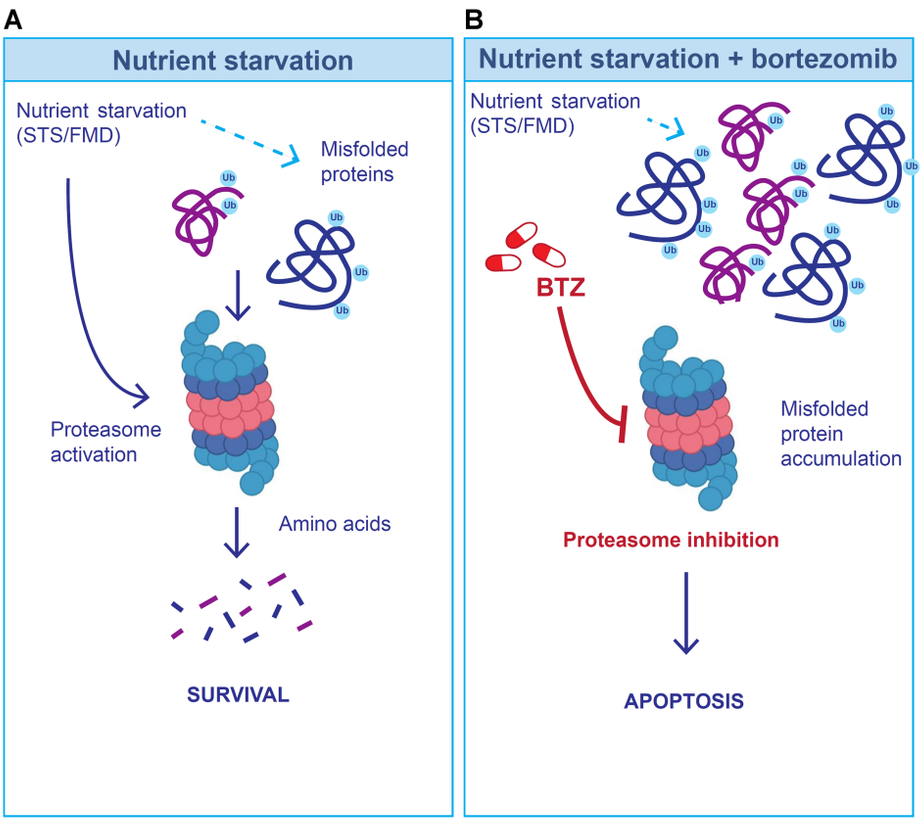

Figure 7.

Hypothetical model to explain the cooperative anti-CLL effect of fasting/FMD and bortezomib (BTZ). **A,** Because nutrient starvation slows down protein synthesis, at least in part as a result of reduced extracellular insulin and IGF1 concentration, it could result in the accumulation of misfolded proteins, which are degraded via the proteasome. **B,** When the proteasome is inhibited (through bortezomib) during starvation conditions, misfolded proteins cannot be timely degraded, and they may accumulate in the cytoplasm, with the results of an increased CLL cell toxicity.

intravenous and subcutaneous mouse CLL models, thus resulting in meaningful prolongation of animal survival.

In *in vitro* experiments, we used two human CLL cell lines obtained from the same patient at different stages of disease progression, namely MEC1 and MEC2 cells (34, 35). Both these CLL lines bear mutations in the *TP53* tumor suppressor gene, which represent the worst prognostic factor in CLL, and which are associated with resistance to most available pharmacologic treatments, including anti-CD20-based chemotherapy regimens (13, 20). In these cell lines, combining nutrient starvation with bortezomib resulted in synergistic antitumor effects. These results were recapitulated in murine L1210 CLL cells, which is also characterized by P53 loss of function.

Bortezomib is the first-in-class proteasome inhibitor approved in the United States and Europe for the treatment of multiple myeloma and mantle cell lymphoma (43, 44). While proteasome inhibitors have been initially considered to have limited activity against CLL (45), recent studies revealed promising anti-CLL activity of bortezomib/-carfilzomib in combination with ibrutinib or other anti-CLL compounds (27, 28), and prospective trials are currently exploring their clinical efficacy (NCT00295932 trial).

To explain the observed cooperative *in vitro* and *in vivo* anti-CLL effects of fasting/FMD and bortezomib + rituximab, we hypothesize that the activation of the proteasome during nutrient deprivation can help CLL cells to degrade misfolded/damaged proteins, which can be toxic to cells, but whose degradation is a source of metabolites that fuel cancer cell growth (**Fig. 7A**). Thus, proteasome inhibition may prevent the degradation of misfolded/damaged proteins required for survival and growth during fasting/FMD, thus precipitating leukemic cell death (**Fig. 7B**). In our experiments, bortezomib treatment, which caused meaningful proapoptotic *in vitro* and *in vivo* effects, also caused an accumulation of CLL cells in the G2/MG_2–M phase of the cell cycle. However, G_2–M arrest/delay is unlikely to explain the anti-CLL effects of bortezomib. Indeed, STS, which caused additive cytotoxic effects in combination with bortezomib, completely reversed bortezomib-induced G_2–M phase accumulation of CLL cells.

Becaue cyclic FMD is a low-cost and safe dietary intervention (7–9, 46), results of our study pave the way for investigating the FMD-bortezomib (± rituximab) combination as a well-tolerated, economically affordable and effective experimental treatment for patients with p53-defective CLL, which is the most aggressive and treatment-resistant CLL subtype. The protective effect of fasting/FMD from bortezomib-induced cytotoxicity in normal cells, as well as the good tolerability of the fasting/FMD-bortezomib-rituximab combination in mice (e.g., full recovery of body weight after fasting/FMD, and lack of progressive body weigth; absence of toxic deaths), is consistent with a generally protective effect of FMD, and it expands the spectrum of chemical compounds of which fasting/FMD could improve the therapeutic index.

Previous *in vitro* studies with a wide range of human B-cell non-Hodgkin lymphoma cell lines have revealed the ability of rituximab to downregulate expression of the antiapoptotic protein Bcl-xL, while enhancing apoptosis (47, 48). In our experiments, rituximab was poorly active against CLL cells, and STS only partially improved its activity. This result could depend on the TP53-mutant status or other cellular characteristics that render certain leukemic cells relatively resistant to anti-CD20–induced apoptosis *in vitro* (20).

In vivo instead, antitumor activity exerted by rituximab is mediated by ADCC as well as complement-dependent cytotoxicity (CDC; refs. 47, 49–52). Our *in vivo* transplantation experiments using B-/T-/NK cell–deficient mice as recipients postulate the involvement

of CDC in combination with fasting/FMD in rituximab-targeted elimination of CLL. Notably, bortezomib was previously shown to increase CD20 expression in rituximab-resistant cell lines (53), possibly explaining the observed *in vivo* antitumor effects of bortezomib and rituximab, in line with studies on follicular lymphoma and mantle cell lymphoma (54, 55).

In tumor-bearing mice, fasting/FMD reduces blood glucose and insulin/IGF-I concentration, thus altering nutrient signaling pathways. While in some tumors blood insulin/IGF-I reduction results in PI3K/AKT/mTORC1/S6K axis inhibition at the tumor level (56), in other tumor models the PI3K/AKT/mTORC1 pathway is activated by cancer cells in response to starvation in an attempt to compensate for nutrient deprivation (4). Here, we showed that starvation-induced inhibition of the IGF1/IGFR-1 axis plays an important role in the anti-CLL effects of fasting/FMD. These data are in line with results of experiments conducted in hormone receptor–positive, human epidermal growth factor receptor 2 (HER2)-positive breast cancer (HR^+ $HER2^-$ BC) models, in which the antitumor effects of fasting/FMD in combination with endocrine therapies ($\pm$ CDK4/6 inhibitors) are mostly mediated by starvation-induced reduction of extracellular insulin, IGF1 and leptin (3). Of note, we recently showed that cyclic FMD not only reduces blood IGF1 concentration, but it also downregulates IGFR1 expression and phosphorylation (i.e., activation) at the tumor level in patients with breast cancer, thus indicating that changes in blood growth factors (systemic metabolic response) is reflected by consistent inhibition of the corresponding signaling pathways in cancer cells (7). These findings could be especially relevant in specific tumor types, such as CLL, in which FMD-induced reduction of blood growth factors contributes to its antitumor effects.

In this study, we reported on the effects of eight consecutive FMD cycles on peripheral blood lymphocyte counts in two patients with CLL undergoing FMD without concomitant systemic therapies. Of note, the fact that after 5–6 years of "watch and wait" approach (with the exception of 8 FMD cycles) these two patients have not yet necessitated systemic anti-CLL treatment initiation is a promising finding, and it is in line with our preclinical findings showing fasting/FMD ability to slow down CLL progression. On the other hand, the fact that these two patients underwent slow, but progressive increase of peripheral blood lymphocytes can be explained by the absence of long-term effects of cyclic FMD when used alone or, alternatively, by the fact that eight FMD cycles may be insufficient to produce long-term disease control in a chronic disease such as CLL. However, because these paients discontinued the use of FMD after 8 cycles, our clinical data do not rule out that continuing periodic use of FMD could extend the duration of "watch and wait period," that is, of the time-to-first use of pharmacologc therapy. Cyclic FMD followed by normocaloric refeeding has been recently shown to be safe, well tolerated, and not associated with progressive weight loss in patients with different tumor types, including advanced and deadly malignancies that often cause sarcopenia or cachexia, such as metastatic pancreatic carcinoma, small-cell lung carcinoma (SCLC), and colorectal carcinoma (7, 8, 10). Different from the case of these malignancies, weight loss, sarcopenia or cachexia rarely occur in patients with CLL, who often present as overweight. For these reasons, we are confident that cyclic FMD can be tolerated by CLL also beyond 8 consecutive cycles. Therefore, future clinical trials evaluating the antitumor effects of cyclic FMD in CLL patients should use a higher number of FMD cycles, alone or in combination with standard anti-CLL therapies.

On the basis of results of our study, we can envision two different clinical scenarios in which the FMD could have therapeutic potential in CLL treatment: (i) patients with indolent CLL who are candidate to a "watch and wait strategy": in these patients, cyclic FMD could be used to control peripheral blood CLL cell expansion and to prevent lymphoid organ infiltration, thus delaying disease progression and the initiation of pharmacologic treatments. On the basis of our preclinical and clinical data, prolonged cyclic FMD (i.e., beyond 8 cycles in patients) might be necessary to achieve long-term control in a chronic disease such as CLL; (ii) patients with aggressive (e.g., *TP53*-mutated) CLL that progresses on first-line regimens: in these patients, the FMD-bortezomib-rituximab combination could be investigated as a new, experimental second- or third-line treatment strategy after BTK inhibitor–containing lines of therapy.

The main limitations of this study consist in: (i) the very low number of patients with CLL included, which does not allow us to draw any conclusions about the antitumor activity or efficacy of cyclic FMD alone in CLL patients; (ii) the use of immunocompromised (NSG) CLL mouse models for *in vivo* experiments, which did not allow us to explore the contribution of antitumor immunity in the observed antitumor effects of fasting and FMD in both systemic and subcutaneous CLL models; (iii) the fact that we combined rituximab and patients as a backbone pharmacologic treatment in *in vivo* experiments, which did not allow us to separately evaluate the antitumor effects of these treatments in combination with fasting/FMD.

In conclusion, cyclic fasting/FMD, which is safe in mouse CLL models and in CLL patients, cooperates with BTZ-RTX to slow down CLL progression and to prolong animal survival by activating apoptosis in CLL cells. Clinical trials with appropriate statistic design in specific CLL patient cohorts are needed to test if cyclic FMD can delay disease progression when used alone in patients with low-risk CLL, and if it can synergize with standard therapies in patients with aggressive disease not responding to standard therapies. Our findings point to FMD plus BTZ-RTZ as a new therapeutic approach that merits clinical evaluation in CLL patients.

Authors' Disclosures

F. Raucci reports a patent for PCT/EP2016/072467 pending. C. Vernieri reports personal fees and other support from Novartis and Eli Lilly; other support from Pfizer, Menarini, and Daiichi Sankyo; personal fees from Istituto Gentili, Accademia di Medicina, and grants from Roche outside the submitted work; in addition, C. Vernieri has a patent for coinvention of "Preparazione alimentare a basso contenuto calorico per l'alimentazione di pazienti affetti da neoplasie"; Italian patent released [first deposited Italian patent n. 102019000009954 (24th June 2019); Extension PCT WO 2020/261131 24th June 2020; European Patent n. 20740399 (pending); Canadian patent n. 2,144,217 (pending); coinventor of Preparazione alimentare per 2019 alimentazione di pazienti oncologici avente un ridotto apporto calorico; international patent request n. PCT/IT2020/000083. Deposited on Dec 17, 2020 (pending)]. M. Di Tano reports a patent 20210352950 pending. R. Buono reports a patent for Fasting-Mimicking Diet Promotes Cancer-Free Survival In Acute Lymphoblastic Leukemia MODELS pending. F. de Braud reports personal fees from Bristol Myers Squibb, Roche, Merck & Co, Bayer, Ignyta, Dephaforum, Biotechespert, Pfizer, Nadirex, Ambrosetti, Incyte, Motore Sanité, Events, Fare Comunicazione, Itanet, ESO, Ambrosetti, Accmed, Idea-z, Dynamicom Education, Tiziana Life Sciences, Celgene, Novartis, Pharm Research Associated, Daiichi Sankyo, Ignyta, Pfizer, Octimet Oncology, Pierre Fabre, Eli Lilly, Roche, AstraZeneca, Gentili, Fondazione Menarini, Sanofi, Taiho, Pierre Fabre, NMS, The healthcare business of Merck KGaA, Darmstadt, Kymab, Pfizer, and Tesaro; other support from Novartis, F. Hoffmann-LaRoche Ltd., Bristol Myers Squibb, Ignyta Operating Inc., Merck Sharp & Dohme Spa, Kymab, Pfizer, Tesaro, MSD, MedImmune LCC, Exelixis Inc., LOXO Oncology Incorporated, DAICHI SANKIO Dev. Limited, Basilea Pharmaceutica International AG, Janssen-Cilag International NV, Merck KGAA; personal fees and other support from Bristol Myers Squibb, Pierre Fabre, Mattioli 1885, MCCann Health, MSD, IQVIA; other support from Bristol Myers Squibb, Roche, Celgene, Amgen, and Sanofi outside the submitted work. V.D. Longo reports grants from AIRC during the conduct of the study; nonfinancial support from L-Nutra outside the submitted work; in addition, V. D. Longo has a patent for 15/761,287 pending. No disclosures were reported by the other authors.

Authors' Contributions

F. Raucci: Conceptualization, formal analysis, supervision, validation, investigation, methodology, writing–original draft, writing–review and editing. **C. Vernieri:** Conceptualization, formal analysis, supervision, validation, investigation, methodology, writing–original draft, writing–review and editing. **M. Di Tano:** Formal analysis, validation, investigation, methodology. **F. Ligorio:** Formal analysis, validation, investigation, methodology. **O. Blaževitš:** Formal analysis, validation, investigation, methodology, writing–original draft, writing–review and editing. **S. Lazzeri:** Formal analysis, validation, investigation, methodology. **A. Shmahala:** Formal analysis, validation, investigation, methodology. **G. Fragale:** Formal analysis, validation, investigation, methodology. **G. Salvadori:** Formal analysis, validation, investigation. **G. Varano:** Formal analysis, validation. **S. Casola:** Investigation. **R. Buono:** Formal analysis, investigation. **E. Visco:** Formal analysis, investigation. **F. de Braud:** Formal analysis, investigation. **V.D. Longo:** Conceptualization, resources, supervision, funding acquisition, writing–review and editing.

Acknowledgments

This study was funded in part by in part by the Associazione Italiana per la Ricerca sul Cancro (AIRC, IG#17605 and IG 21820) and in part by the kind donation of Simon McDonald (to V.D. Longo). C. Vernieri. was supported by the Italian Association for Cancer Research (MFAG # 22977). S. Casola was supported by the Italian Association for Cancer Research (AIRC, IG# 23747). G. Varano was supported by the European Union's Horizon 2020 research and innovation programme under the Marie Skłodowska-Curie grant agreement No 895887. G. Fragale was supported by the Italian Association for Cancer Research (AIRC Fellowship for Italy#28149). The authors would like to thank Dr. Sara Martone and Dr. Maria Grazia Totaro (IFOM Flow Cytometry Core Facility) for assistance in the FACS analysis; Dr. Federica Pisati (IFOM histologic facility) for the assistance in histologic preparation of the samples; Drs. Stefania Lavore, Ilaria Rancati and Cinzia Cancellieri (IFOM Cell Culture Core Facility), Dr. Martina Milani (IEO, Institute of European Oncology) and the Pharmacy at INT, and in particular Drs. Marta Del Vecchio, Margherita Galassi, and Vito Ladisa for providing bortezomib and rituximab used in this study, and Dr. Celeste Ungaro for her administrative support.

Note

Supplementary data for this article are available at Cancer Research Online (http://cancerres.aacrjournals.org/).

Received February 1, 2023; revised October 12, 2023; accepted January 18, 2024; published first January 19, 2024.

References

1. Lee C, Raffaghello L, Brandhorst S, Safdie FM, Bianchi G, Martin-Montalvo A, et al. Fasting cycles retard growth of tumors and sensitize a range of cancer cell types to chemotherapy. Sci Transl Med 2012;4:124ra27.
2. Di Biase S, Lee C, Brandhorst S, Manes B, Buono R, Cheng CW, et al. Fasting-mimicking diet reduces HO-1 to promote T cell-mediated tumor cytotoxicity. Cancer Cell 2016;30:136–46.
3. Caffa I, Spagnolo V, Vernieri C, Valdemarin F, Becherini P, Wei M, et al. Fasting-mimicking diet and hormone therapy induce breast cancer regression. Nature 2020;583:620–4.
4. Salvadori G, Zanardi F, Iannelli F, Lobefaro R, Vernieri C, Longo VD. Fasting-mimicking diet blocks triple-negative breast cancer and cancer stem cell escape. Cell Metab 2021;33:2247–59.
5. Di Tano M, Raucci F, Vernieri C, Caffa I, Buono R, Fanti M, et al. Synergistic effect of fasting-mimicking diet and vitamin C against KRAS mutated cancers. Nat Commun 2020;11:2332.
6. Ajona D, Ortiz-Espinosa S, Lozano T, Exposito F, Calvo A, Valencia K, et al. Short-term starvation reduces IGF-1 levels to sensitize lung tumors to PD-1 immune checkpoint blockade. Nat Cancer 2020;1:75–85.
7. Vernieri C, Fucà G, Ligorio F, Huber V, Vingiani A, Iannelli F, et al. Fasting-mimicking diet is safe and reshapes metabolism and antitumor immunity in patients with cancer. Cancer Discov 2022;12:90–107.
8. Valdemarin F, Caffa I, Persia A, Cremonini AL, Ferrando L, Tagliafico L, et al. Safety and feasibility of fasting-mimicking diet and effects on nutritional status and circulating metabolic and inflammatory factors in cancer patients undergoing active treatment. Cancers 2021;13:4013.
9. de Groot S, Lugtenberg RT, Cohen D, Welters MJP, Ehsan I, Vreeswijk MPG, et al. Fasting mimicking diet as an adjunct to neoadjuvant chemotherapy for breast cancer in the multicentre randomized phase 2 DIRECT trial. Nat Commun 2020;11:3083.
10. Ligorio F, Fuca G, Provenzano L, Lobefaro L, Zanenga L, Vingiani A, et al. Exceptional tumor responses to fasting-mimicking diet combined with standard anticancer therapies: a sub-analysis of the NCT03340935 trial. Eur J Cancer 2022;172:300–10.
11. Ligorio F, Lobefaro R, Fucà G, Provenzano L, Zanenga L, Nasca V, et al. Adding fasting-mimicking diet to first-line carboplatin-based chemotherapy is associated with better overall survival in advanced triple-negative breast cancer patients: A subanalysis of the NCT03340935 trial. Int J Cancer 2023;154:114–123.
12. Chiorazzi N, Rai KR, Ferrarini M. Chronic lymphocytic leukemia. N Engl J Med 2005;352:804–15.
13. Kipps TJ, Stevenson FK, Wu CJ, Croce CM, Packham G, Wierda WG, et al. Chronic lymphocytic leukaemia. Nat Rev Dis Primers 2017;3:16096.
14. Hallek M, Cheson BD, Catovsky D, Caligaris-Cappio F, Dighiero G, Dohner H, et al. iwCLL guidelines for diagnosis, indications for treatment, response assessment, and supportive management of CLL. Blood 2018;131:2745–60.
15. Brown JR, O'Brien S, Kingsley CD, Eradat H, Pagel JM, Lymp J, et al. Obinutuzumab plus fludarabine/cyclophosphamide or bendamustine in the initial therapy of CLL patients: the phase 1b GALTON trial. Blood 2015;125:2779–85.
16. Gentile M, Zirlik K, Ciolli S, Mauro FR, Di Renzo N, Mastrullo L, et al. Combination of bendamustine and rituximab as front-line therapy for patients with chronic lymphocytic leukaemia: multicenter, retrospective clinical practice experience with 279 cases outside of controlled clinical trials. Eur J Cancer 2016;60:154–65.
17. Eichhorst B, Fink AM, Bahlo J, Busch R, Kovacs G, Maurer C, et al. First-line chemoimmunotherapy with bendamustine and rituximab versus fludarabine, cyclophosphamide, and rituximab in patients with advanced chronic lymphocytic leukaemia (CLL10): an international, open-label, randomised, phase 3, non-inferiority trial. Lancet Oncol 2016;17:928–42.
18. Goede V, Fischer K, Busch R, Engelke A, Eichhorst B, Wendtner CM, et al. Obinutuzumab plus chlorambucil in patients with CLL and coexisting conditions. N Engl J Med 2014;370:1101–10.
19. Hillmen P, Robak T, Janssens A, Babu KG, Kloczko J, Grosicki S, et al. Chlorambucil plus ofatumumab versus chlorambucil alone in previously untreated patients with chronic lymphocytic leukaemia (COMPLEMENT 1): a randomised, multicentre, open-label phase 3 trial. Lancet 2015;385:1873–83.
20. Hallek M, Fischer K, Fingerle-Rowson G, Fink AM, Busch R, Mayer J, et al. Addition of rituximab to fludarabine and cyclophosphamide in patients with chronic lymphocytic leukaemia: a randomised, open-label, phase 3 trial. Lancet 2010;376:1164–74.
21. Byrd JC, Brown JR, O'Brien S, Barrientos JC, Kay NE, Reddy NM, et al. Ibrutinib versus ofatumumab in previously treated chronic lymphoid leukemia. N Engl J Med 2014;371:213–23.
22. Burger JA, Tedeschi A, Barr PM, Robak T, Owen C, Ghia P, et al. Ibrutinib as initial therapy for patients with chronic lymphocytic leukemia. N Engl J Med 2015;373:2425–37.
23. Sharman JP, Egyed M, Jurczak W, Skarbnik A, Pagel JM, Flinn IW, et al. Acalabrutinib with or without obinutuzumab versus chlorambucil and obinutuzmab for treatment-naive chronic lymphocytic leukaemia (ELEVATE TN): a randomised, controlled, phase 3 trial. Lancet 2020;395:1278–91.
24. Tam CS, Robak T, Ghia P, Kahl BS, Walker P, Janowski W, et al. Zanubrutinib monotherapy for patients with treatment naive chronic lymphocytic leukemia and 17p deletion. Haematologica 2020;106:2354–63.
25. Seymour JF, Kipps TJ, Eichhorst B, Hillmen P, D'Rozario J, Assouline S, et al. Venetoclax-rituximab in relapsed or refractory chronic lymphocytic leukemia. N Engl J Med 2018;378:1107–20.

26. Wilson WH. Progress in chronic lymphocytic leukemia with targeted therapy. N Engl J Med 2016;374:386–8.
27. Gupta SV, Hertlein E, Lu Y, Sass EJ, Lapalombella R, Chen TL, et al. The proteasome inhibitor carfilzomib functions independently of p53 to induce cytotoxicity and an atypical NF-kappaB response in chronic lymphocytic leukemia cells. Clin Cancer Res 2013;19:2406–19.
28. Lamothe B, Cervantes-Gomez F, Sivina M, Wierda WG, Keating MJ, Gandhi V. Proteasome inhibitor carfilzomib complements ibrutinib's action in chronic lymphocytic leukemia. Blood 2015;125:407–10.
29. Baou M, Kohlhaas SL, Butterworth M, Vogler M, Dinsdale D, Walewska R, et al. Role of NOXA and its ubiquitination in proteasome inhibitor-induced apoptosis in chronic lymphocytic leukemia cells. Haematologica 2010;95:1510–8.
30. Rozovski U, Hazan-Halevy I, Barzilai M, Keating MJ, Estrov Z. Metabolism pathways in chronic lymphocytic leukemia. Leuk Lymphoma 2016;57:758–65.
31. Tsai HT, Cross AJ, Graubard BI, Oken M, Schatzkin A, Caporaso NE. Dietary factors and risk of chronic lymphocytic leukemia and small lymphocytic lymphoma: a pooled analysis of two prospective studies. Cancer Epidemiol Biomarkers Prev 2010;19:2680–4.
32. Brandhorst S, Choi IY, Wei M, Cheng CW, Sedrakyan S, Navarrete G, et al. A periodic diet that mimics fasting promotes multi-system regeneration, enhanced cognitive performance, and healthspan. Cell Metab 2015;22:86–99.
33. Brandhorst S, Wei M, Hwang S, Morgan TE, Longo VD. Short-term calorie and protein restriction provide partial protection from chemotoxicity but do not delay glioma progression. Exp Gerontol 2013;48:1120–8.
34. Agathangelidis A, Scarfo L, Barbaglio F, Apollonio B, Bertilaccio MT, Ranghetti P, et al. Establishment and characterization of PCL12, a novel CD5+ chronic lymphocytic leukaemia cell line. PLoS One 2015;10:e0130195.
35. Stacchini A, Aragno M, Vallario A, Alfarano A, Circosta P, Gottardi D, et al. MEC1 and MEC2: two new cell lines derived from B-chronic lymphocytic leukaemia in prolymphocytoid transformation. Leuk Res 1999;23:127–36.
36. Pozzo F, Dal Bo M, Peragine N, Bomben R, Zucchetto A, Rossi F, et al. Detection of TP53 dysfunction in chronic lymphocytic leukemia by an in vitro functional assay based on TP53 activation by the non-genotoxic drug Nutlin-3: a proposal for clinical application. J Hematol Oncol 2013;6:83.
37. Cory AH, Chen J, Cory JG. Effects of PRIMA-1 on wild-type L1210 cells expressing mutant p53 and drug-resistant L1210 cells lacking expression of p53: necrosis vs. apoptosis. Anticancer Res 2006;26:1289–95.
38. Lee C, Safdie FM, Raffaghello L, Wei M, Madia F, Parrella E, et al. Reduced levels of IGF-I mediate differential protection of normal and cancer cells in response to fasting and improve chemotherapeutic index. Cancer Res 2010; 70:1564–72.
39. Ling YH, Liebes L, Jiang JD, Holland JF, Elliott PJ, Adams J, et al. Mechanisms of proteasome inhibitor PS-341-induced G(2)-M-phase arrest and apoptosis in human non-small cell lung cancer cell lines. Clin Cancer Res 2003;9:1145–54.
40. Bertilaccio MT, Scielzo C, Simonetti G, Ponzoni M, Apollonio B, Fazi C, et al. A novel Rag2-/-gammac-/–xenograft model of human CLL. Blood 2010;115: 1605–9.
41. Caffa I, D'Agostino V, Damonte P, Soncini D, Cea M, Monacelli F, et al. Fasting potentiates the anticancer activity of tyrosine kinase inhibitors by strengthening MAPK signaling inhibition. Oncotarget 2015;6:11820–32.
42. Lu Z, Xie J, Wu G, Shen J, Collins R, Chen W, et al. Fasting selectively blocks development of acute lymphoblastic leukemia via leptin-receptor upregulation. Nat Med 2017;23:79–90.
43. Scott K, Hayden PJ, Will A, Wheatley K, Coyne I. Bortezomib for the treatment of multiple myeloma. Cochrane Database Syst Rev 2016;4:CD010816.
44. Robak P, Robak T. Bortezomib for the treatment of hematologic malignancies: 15 years later. Drugs R D 2019;19:73–92.
45. Faderl S, Rai K, Gribben J, Byrd JC, Flinn IW, O'Brien S, et al. Phase II study of single-agent bortezomib for the treatment of patients with fludarabine-refractory B-cell chronic lymphocytic leukemia. Cancer 2006; 107:916–24.
46. Wei M, Brandhorst S, Shelehchi M, Mirzaei H, Cheng CW, Budniak J, et al. Fasting-mimicking diet and markers/risk factors for aging, diabetes, cancer, and cardiovascular disease. Sci Transl Med 2017;9:eaai8700.
47. Jazirehi AR, Gan XH, De Vos S, Emmanouilides C, Bonavida B. Rituximab (anti-CD20) selectively modifies Bcl-xL and apoptosis protease activating factor-1 (Apaf-1) expression and sensitizes human non-Hodgkin's lymphoma B cell lines to paclitaxel-induced apoptosis. Mol Cancer Ther 2003;2: 1183–93.
48. Stolz C, Hess G, Hähnel PS, Grabellus F, Hoffarth S, Schmid KW, et al. Targeting Bcl-2 family proteins modulates the sensitivity of B-cell lymphoma to rituximab-induced apoptosis. Blood 2008;112:3312–21.
49. Di Gaetano N, Cittera E, Nota R, Vecchi A, Grieco V, Scanziani E, et al. Complement activation determines the therapeutic activity of rituximab in vivo. J Immunol 2003;171:1581–7.
50. Kennedy AD, Solga MD, Schuman TA, Chi AW, Lindorfer MA, Sutherland WM, et al. An anti-C3b(i) mAb enhances complement activation, C3b(i) deposition, and killing of CD20+ cells by rituximab. Blood 2003;101:1071–9.
51. Lara S, Heilig J, Virtanen A, Kleinau S. Exploring complement-dependent cytotoxicity by rituximab isotypes in 2D and 3D-cultured B-cell lymphoma. BMC Cancer 2022;22:678.
52. van Meerten T, van Rijn RS, Hol S, Hagenbeek A, Ebeling SB. Complement-induced cell death by rituximab depends on CD20 expression level and acts complementary to antibody-dependent cellular cytotoxicity. Clin Cancer Res 2006;12:4027–35.
53. Bil J, Winiarska M, Nowis D, Bojarczuk K, Dabrowska-Iwanicka A, Basak GW, et al. Bortezomib modulates surface CD20 in B-cell malignancies and affects rituximab-mediated complement-dependent cytotoxicity. Blood 2010;115: 3745–55.
54. Zinzani PL, Khuageva NK, Wang H, Garicochea B, Walewski J, Van Hoof A, et al. Bortezomib plus rituximab versus rituximab in patients with high-risk, relapsed, rituximab-naive or rituximab-sensitive follicular lymphoma: subgroup analysis of a randomized phase 3 trial. J Hematol Oncol 2012;5:67.
55. Fan WH, Wang FL, Lu ZH, Pan ZZ, Li LR, Gao YH, et al. Surgery with versus without preoperative concurrent chemoradiotherapy for mid/low rectal cancer: an interim analysis of a prospective, randomized trial. Chin J Cancer 2015;34: 394–403.
56. Cheng CW, Adams GB, Perin L, Wei M, Zhou X, Lam BS, et al. Prolonged fasting reduces IGF-1/PKA to promote hematopoietic-stem-cell-based regeneration and reverse immunosuppression. Cell Stem Cell 2014;14:810–23.